http://dx.doi.org/10.5012/bkcs.2014.35.4.1005

Fullerene Dimers Connected through C_{24} and C_{36} Bridge Cages

Maryam Anafcheh and Reza Ghafouri*

*Department of Chemistry, Shahr-e-Ray Branch, Islamic Azad University, Tehran, Iran. *E-mail: reghafouri@gmail.com*
Received September 7, 2013, Accepted December 5, 2013

We have performed DFT calculations to devise some possible fullerene dimers (from C_{60} and C_{80}) connected through C_{24} and C_{36} bridge cages with the face-to-face linking model. The fullerene dimers with C_{36} bridges have lower binding energies and greater HOMO-LUMO gaps than those of the fullerene dimers with C_{24} bridges. Also, the replacement of C_{60} cages with C_{80} ones always leads to an increase in binding energies and HOMO-LUMO gaps in these systems. Dimerization of C_{60} and C_{80} fullerenes with C_{24} and C_{36} results in a significant decrease in antiaromaticity of the antiaromatic cages C_{24} and C_{80}, and an increase in the aromaticity of the aromatic cages C_{36} and C_{60}. Therefore, DFT results indicate that those fullerene dimers involving the initially harshly antiaromatic C_{24} or C_{80} cages are more energetically favorable configuration than the fullerene dimers involving the aromatic C_{36} and C_{60} cages.

Key Words : Fullerene dimers, NICS, HOMO–LUMO gap, Binding energy, DFT

Introduction

The understanding of chemical reactivity of buckminsterfullerene (C_{60}),[1] and other smaller and larger fullerenes would lead to the synthesis of a large number of fullerene derivatives whose properties and applications have been extensively investigated from many viewpoints.[1-5] One of the unique aspects of fullerenes in this field is the formation of interfullerene bondings, which makes a rich variety of nanoscale network structures such as dimers, oligomers, and one- and two-dimensional fullerene polymeric materials.[6-11] In general, it has been suggested that interaction between two fullerene cages can arise through one of the four possible approaches: C-C bond between C_{60} cages forming a [1+1] dimer (point-point mode); C=C bond forming a [2+2] dimer (side-side mode); forming a [5+5] dimer by face-face mode between two pentagons; and forming a [6+6] dimer by face-face mode between two hexagons.[12] In recent years, more attention has been paid to fullerene dimers because their unique physical and chemical properties provide intriguing possibilities as model compounds for nano- and polymer science, and offer potential access to novel molecular electronic devices.[13,14] In this respect, a series of fullerene dimers have been produced, such as C_{120},[15] the carbon-bridged dimers: C_{121},[16-19] C_{140}, C_{131},[20] and C_{122},[15,19,21] and the heteroatom bridged dimer: $C_{120}O$,[22-24] which could be used as the basic units of fullerene chain structures. The simplest fullerene dimer C_{120}, $(C_{60})_2$, has been prepared by solid-state[25] and by chemical methods. On the other hand, Osterodt and Vogtle,[26] Fabre *et al.*,[27] and Dragoe *et al.*[28] isolated the C_{122} consisting of C_{60} fullerenes joined by a (C=C) bridge with sp^2-hybridized C atoms which are added across C_{60} bonds shared by two hexagons (hexagon-hexagon bonds). Forman *et al*.[29] reported the first experimental synthesis and characterization of five [2+2] structural isomers of fullerene dimers C_{140}. The C_{131} is the first hybrid type of the dumbbell-like fullerene dimer that consists of two different sizes of cages, C_{60} and C_{70}, with a central atom-bridge.[20] Its formation, structure and properties may be more complicated and interesting than those of C_{121} or C_{141}.[16-20] Shvartsburg *et al.*[30] used the chain of C2 units to design dimers of original fullerenes (C_{60} or C_{70}). Finally, Manaa,[31] and Anafcheh and Ghafouri[32] proposed carbon and BN hexagons (benzene-like unit) as a building block for connecting between two C_{60} fullerene cages in order to yield unique electronic properties.

As mentioned above, it has been shown that fullerenes also react with themselves to generate fullerene dimers. Since carbon cages smaller than C_{60} violate the isolated pentagon rule (IPR), they have higher strain and reactivity due to the adjacent pentagons, thus they are good candidates to form dimers, polymers and solids.[33] With this initial thought in mind, in this article we consider small fullerenes such as C_{24} and C_{36} as molecular bridges for joining higher fullerenes such as C_{60} and C_{80}, for the first time, see Figure 1. Then we investigate their electronic and magnetic properties in comparison to those of their parents by calculating HOMO–LUMO gaps, binding energies, and NICS indices. In fact, the synthesis and characterization of such fullerene dimers are of main interest due to their unique structural, magnetic, superconducting and mechanical properties,[7,9] which are considerably different from those of other carbon nanostructures such as carbon nanotubes and fullerene cages. Since the considered fullerenes in this study are borderless polycyclic conjugated systems with internal cavities, endohedral ^{3}He NMR chemical shifts have proven to be a useful tool for characterizing them and their derivatives.[34-36] Determining the chemical shift of encapsulated ^{3}He nucleus into a fullerene cage and comparing with the ^{3}He chemical shift outside gets a direct measure of the shielding of the magnetic field by the fullerene; such experiments are well known for fullerenes. Providing a good prediction for the endohedral ^{3}He NMR chemical shift, nucleus independent

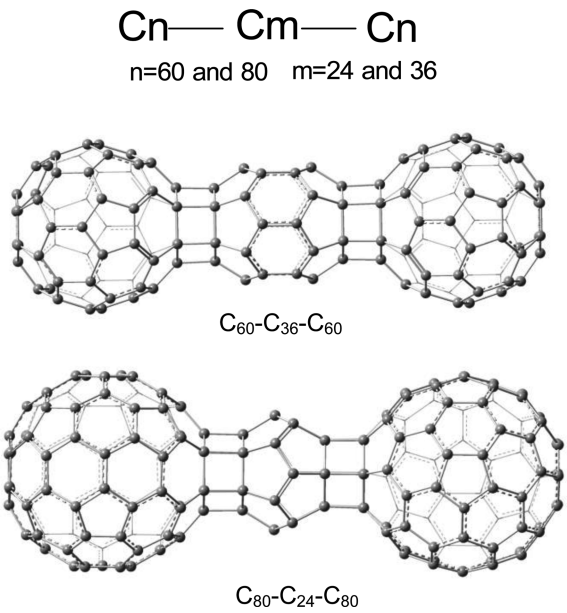

Figure 1. Schematic diagram of fullerene dimers together with the optimized geometries of C_{60}-C_{36}-C_{60} (C_{156}) and C_{80}-C_{24}-C_{80} (C_{184}).

chemical shift (NICS) was proposed by Schleyer *et al.* in 1996.[37] Therefore, in order to probe the local effects of magnetic field inside each fullerene cage we employ grid distribution of NICS inside these molecular clusters and their parents. Magnetic field inside each cage is a consequence of diamagnetism and is related to the induced ring current in the fullerene molecular orbitals, which causes extra stabilization/destabilization in the case of aromatic/antiaromatic compounds.[38] Therefore, it can provide better insights of the electron delocalization, diamagnetic susceptibilities, molecular aromaticity and magnetic properties.

Computational Methods. All density functional theory (DFT) quantum calculations are performed using Gaussian 98 program package.[39] We consider small fullerenes C_{24} and C_{36} as molecular bridges for joining higher fullerenes C_{60} and C_{80}, see Figure 1. Therefore, the structural geometries of six different configurations of the considered models are allowed to relax by all-atomic optimization. Because of the large sizes of the investigated systems optimization method is qualified step by step as follows: first C_{24}, C_{36}, C_{60} and C_{80} fullerene cages considered as the starting points for the design of these compounds are optimized at the B3LYP/6-31G(d) level of theory.[40] In the next step the geometries obtained in step 1 are used to create initial geometries of the fullerene dimers, *i.e.*, smaller fullerenes, C_{24} and C_{36}, are located between two cages with approximate interlayer bond length of 1.6 Å (based on reported CC bond lengths for the fullerene dimers[15,32]); then optimization is first performed with 3-21G basis set for the resulted molecules and finally optimal geometries and normal mode frequencies for all the structures are obtained using standard 6-31G(d) basis set. The coordinates of all the optimized structures can be found in supplementary material. The standard 6-31G(d) basis set is employed due to being affordable and accurate enough for geometry optimization of even large molecules.[40,41] Real frequencies obtained from frequency calculations confirm that all of them are minimum energy structures.

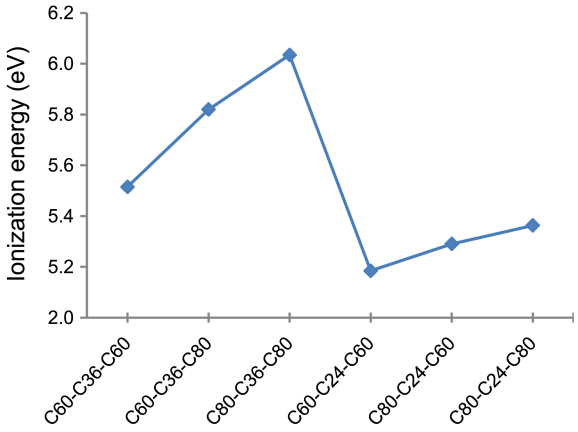

Figure 2. Ionization energy (eV) for the fullerene dimers.

As a stability criterion of different configurations, binding energies per atom have been calculated according to the following expression:

$$E_{bin} = \frac{(nE_C - E_T)}{n}$$

where E_T is the total energy of the fullerene dimers. Systems with larger binding energies are more stable. To calculate the NICS, ghost atoms are placed along the principal axes of the considered fullerene dimers and their parents with a step size of 0.5 Å. The zero point of the coordinate system is positioned at the bridge centers of the optimized structures of the considered fullerene dimers.

Results and Discussion

Geometrical and Stability Properties. We have chosen the C_{60} and C_{80} cages as parent molecules, which are fully optimized at the B3LYP/6-31G* level. The obtained structure of C_{60} is consistent with the literature; the prediction of bond lengths of the hexagon-hexagon (h-h) and hexagon-pentagon (h-p) junctions (1.452 and 1.393 Å, respectively) is in excellent agreement with the experimental values (1.458 and 1.401 Å, respectively).[42,43] The C_{36} and C_{24} fullerene cages are chosen as bridges between two fullerene cages. The structure of C_{24} can be regarded as a [12]trannulene[44] capped with two hexagonal terminal caps. Its optimized structure is indeed affirmative of such a consideration with the uniform C-C bond lengths (1.420 Å) of the hexagonal terminal caps and the much longer C-C bond lengths of 1.530 Å between the hexagonal caps and the central [12]trannulenic ring. Moreover, the localized C=C bond lengths of 1.365 Å and C-C bond lengths of 1.462 Å in the central [12]trannulenic ring are in excellent agreement with the reported experimental values (1.365 and 1.463 Å, respectively).[44,45] The structure of C_{36} fullerene cage has been described in our previous work.[46]

In this work, we use the face-to-face linking model to

Table 1. Total energy (E_T), Binding energy (E_{bin}), and HOMO-LUMO energy gaps (E_g) in the fullerene dimers

Model	E_T	E_{HOMO}	E_{LUMO}	E_g	E_{bin}
C_{60}-C_{36}-C_{60}	-5910.61	-5.51	-4.47	1.05	3.06
C_{60}-C_{36}-C_{80}	-6671.61	-5.82	-4.61	1.21	3.56
C_{80}-C_{36}-C_{80}	-7432.61	-6.03	-4.78	1.26	3.96
C_{60}-C_{24}-C_{60}	-5482.83	-5.18	-4.40	0.78	8.14
C_{80}-C_{24}-C_{60}	-6248.28	-5.29	-4.43	0.86	8.80
C_{80}-C_{24}-C_{80}	-7011.88	-5.37	-4.49	0.88	9.03

create six types of fullerene dimers with C_{24} and C_{36} bridges, see Figure 1. When two neighboring carbon cages share their hexagonal caps with the face-to-face pattern, sp^2 hybridization transfers to sp^3 hybridization for the carbon atoms in the merged region. As the structures are being reported for the first time, their geometrical characteristics are discussed briefly with the aim of giving better interpretations of these clusters. Based on the optimized structures, the intercage bond lengths of six fullerene dimer are in the range 1.603-1.622 Å, which can be compared with the intercage bond lengths of 1.60 Å reported by Fowler *et al.*[47] for a linear chain of D_{6h}-C_{36} cages, and the electron-diffraction pattern of C_{36}-based solid which suggested an intercage distance shorter than 1.7 Å. Moreover, the calculated C-C bond lengths of 1.657-1.660 Å in the two hexagonal terminal caps of C_{24} bridge cages are slightly longer than the corresponding C-C bond lengths (1.522-1.604 Å) in the C_{36} bridge cages.

To compare the obtained results with those available in the literature, binding energies per atom are calculated for the C_{36} and C_{60} fullerenes to be 8.880 and 7.820 eV/atom, which are in agreement with the previously reported values (8.55 and 7.72 eV/atom).[2,45] The little difference observed can be due to the different computational methods used. We first note that binding energies for the fullerene dimers with C_{36} bridges are always lower than those of the fullerene dimers with C_{24} bridges. Secondly, the replacement of C_{60} cages with C_{80} ones (increasing the size of fullerene cage) leads to an increase in binding energy in these systems, see Table 1.

The energy difference between the highest occupied molecular orbital (HOMO) and the lowest unoccupied molecular orbital (LUMO), E_g, indicates that C_{36} and C_{60} are semiconductors with the E_g of 1.02 and 1.66 eV, respectively, which are in agreement with the reported values in the literature (0.8 and 1.8 eV).[45,48] As can be seen in Table 1, in contrast to binding energies, the E_g values of the fullerene dimers with C_{36} bridges are larger than those of the fullerene dimers with C_{24} bridges. This occurrence may bring about a change in the related electrical conductivity since it is well known that the E_g (or band gap in the bulk materials) is a major factor that determines the electrical conductivity of the material. A classic relation between them is as follows[49]:

$$\sigma \propto \exp\left(\frac{-E_g}{2kT}\right)$$

where σ is the electrical conductance and k is the Boltzmann's constant. According to the equation, smaller E_g leads to higher conductance at a given temperature. Therefore, all of the considered models in this study are semiconductors with E_g values of 1.05-1.26 eV when C_{36} cage is located between two fullerene cages and 0.78-0.88 eV when C_{24} is sandwiched between two fullerene cages. Moreover, it is also found that band gaps increase with increasing the size, *i.e.*, replacing C_{60} with C_{80} leads to larger HOMO-LUMO gap for each group of fullerene dimers, see Table 1.

The first ionization potentials (IP) are calculated under the Koopmans' theorem for closed-shell molecules, based on the frozen orbital approximations and the finite difference approach. In the other words, they are expressed in terms of the highest occupied molecular orbital (HOMO) energies, E_{HOMO}: IP ≈ $-E_{HOMO}$. At this point it is necessary to mention that the focus is not to find precise ionization potential values; instead, the primary purpose is to study the evolution and the trend of IP in the considered models, and this is just an approximate comparison. Figure 2 depicts the trend of ionization potential for the considered models. The IP plot indicates that the fullerene dimers with C_{36} bridges have higher ionization potentials compared to the fullerene dimers with C_{24} bridges, and are thus harder to oxidize (oxidation). Meanwhile, replacement of C_{60} cages with C_{80} ones (increasing the size of fullerene cage) leads to an increase in ionization potential in these systems.

NICS Characterization. Aromaticity describes molecules that benefit energetically from the presence of cyclic or spherical electron delocalization in closed circuits of mobile electrons. It is well known that the stability is not directly related to aromatic stabilization but with strain reduction. This is consistent with the high aromaticity of C_{36} compared to the antiaromaticity of C_{24}, as it is measured by the magnetic aromaticity index of nucleus independent chemical shift (NICS) evaluated at the center of the cages.

Since the aromaticity is not an observable characteristic, there is no magnitude that defines it clearly, and so it is generally evaluated indirectly on the basis of energetic, geometric, or electronic criteria. Especially, it can be followed by obtaining information from the magnetic properties. In fact, the most important methods among several ones to evaluate aromaticity are based on NMR chemical shifts and diamagnetic susceptibilities. Compounds with considerably exalted diamagnetic susceptibility are considered as aromatic structures. The ring currents generated in such molecules by an external magnetic field result in special properties such as "exalted" magnetic susceptibilities and NMR chemical shifts displaced from their normal ranges.[37,38] Such particular magnetic influences typically are especially large inside aromatic cyclic or cage-like molecules. To match the familiar NMR convention, NICS indices correspond to the negative of the magnetic shielding, a well-defined property of electronic systems, computed at chosen points designated using the Bq ghost atoms. Significantly negative NICS values in interior positions of cages (magnetically shielded) indicate the presence of induced diatropic ring currents or aromaticity.

On the other hand, antiaromatic cages are identified by

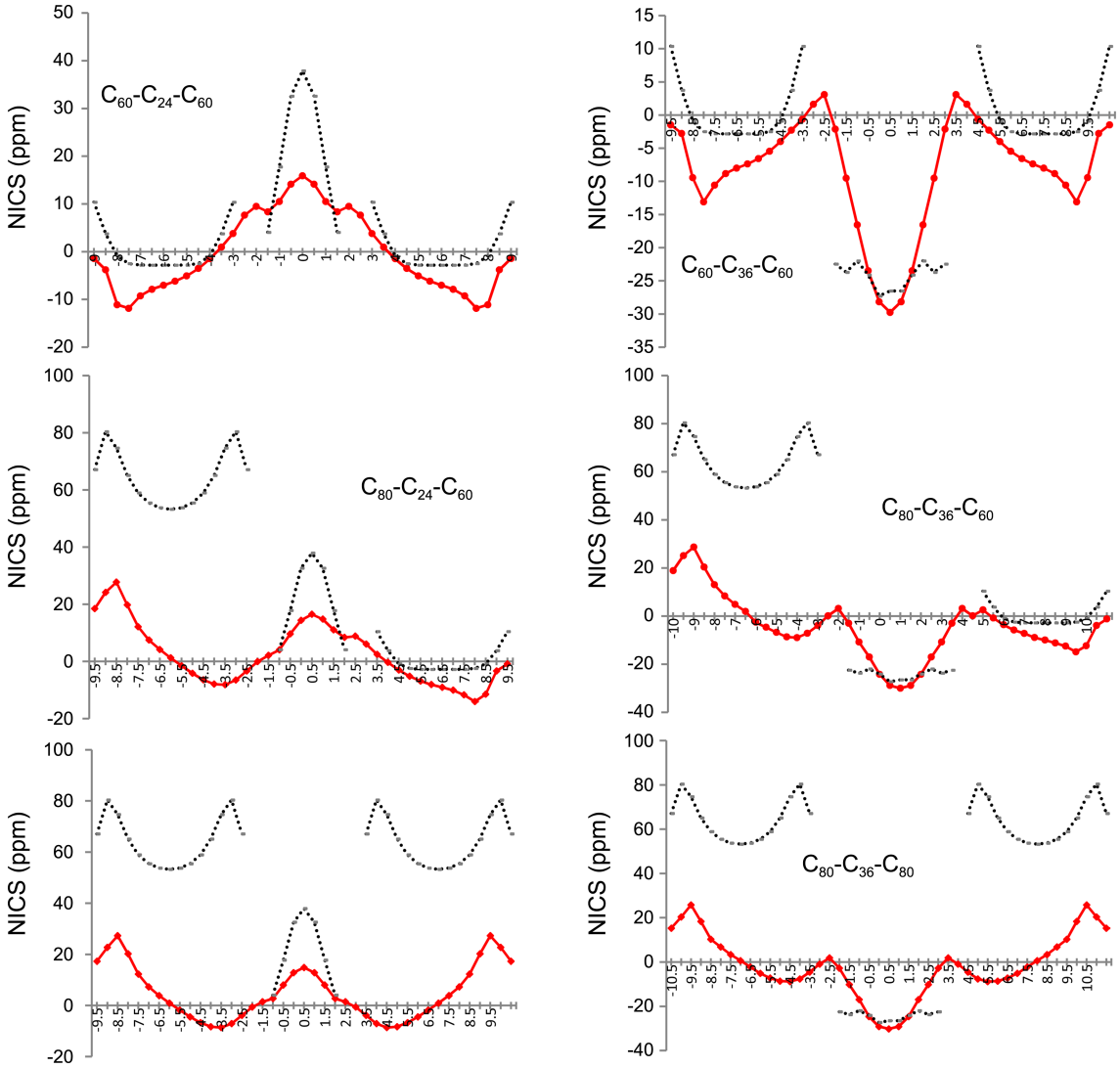

Figure 3. Computed NICS values (ppm) along the principal axes of fullerene dimers connected through C_{24} and C_{36} bridge cages. The zero point of the coordinate system is positioned at the centers of bridge cages.

their positive NICS values (magnetically deshielded), indicating paratropic ring currents.

As mentioned above, C_{24} cage can be regarded as a [12]trannulene capped with two benzene rings at both sides. The local ring currents are diatropic within the six membered rings and, in sharp contrast, paratropic within the [12]trannulenic ring. Compensation of these two local effects results in NICS value of 37.89 ppm at the cage center,[50] so C_{24} fullerene is antiaromatic at all. The C_{36} fullerene cage can be viewed as being made of a zigzag (6, 0) tubular belt, six-membered cyclic polyacene, joined to hexagonal terminal caps, which results in the high aromaticity of the C_{36} with the calculated NICS value of –26.52,[50] in agreement with the experimental value of –28.8 ppm previously reported by Saunders *et al.*.[45]

Figure 3 depicts variations of NICS values *versus* distances from the bridge center for the considered compounds and their parent cages (The calculated NICS values for the fullerene dimers have been shown in Table S1 of the Supplementary material). Dimerization of C_{60} and C_{80} fullerenes with C_{24} and C_{36} significantly change their aromatic characters, leading to a decrease in antiaromaticity of the C_{24} and C_{80} with paratropic characters, while an increase in the aromaticity of the aromatic C_{36} and C_{60} cages. In other words, NICS values reflect substantial differences in magnetic properties at the cage centers of fullerene dimers. For example, weakly diatrophic (aromatic) C_{60} has a moderate NICS value of –2.82 ppm,[50] while it receives more aromaticity with NICS value of –7.35 ppm in the fullerene dimer C_{156} (C_{60}-C_{36}-C_{60}). In this compound NICS in aromatic fullerene C_{36} changes from –26.52 ppm to the value of –29.76 ppm, *i.e.*, aromaticity increases. The inverse behavior is observed for C_{24} and C_{80} which are severely antiaromatic with high positive NICS values of 37.89 and 53.22 ppm, respectively. Compensation between diatropic and paratropic ring currents leads to a decrease in NICS values to 7.16 and 0.93 ppm at the cage centers of C_{24} and C_{80}, respectively, in the fullerene dimer C_{184}(C_{80}-C_{24}-C_{80}). These trends reveal that fullerene dimerization causes major changes in the magnetic properties at

the cage centers.

Now we are interested to make an attempt to correlate the stability of fullerene dimers with their aromaticity character. DFT results indicate that those fullerene dimers involving the initially harshly antiaromatic C_{24} or C_{80} cages are more energetically favorable configuration, with the binding energies of 8.14-9.03 eV/atom, than the fullerene dimers involving C_{36} and C_{60}, with the binding energies of 3.06-3.96 eV/atom. It is noted that the E_{bin} of the fullerene dimer C_{184} (C_{80}-C_{24}-C_{80}) with three antiaromatic cage is larger than those of the other fullerene dimers. Hence, a change in aromaticity character, especially decrease of antiaromaticity, plays a major role in the stability of fullerene dimer. In fact, decrement of antiaromatic character (NICS) inside the joined antiaromatic fullerene cages leads to an increase in the ability of these compounds to sustain an induced ring current, which causes extra stabilization in the case of fullerene dimers of C_{80} fullerene with C_{24} bridge cages. Therefore, it seems that the results of this section and those of stability character in previous section mostly support each other.

Conclusion

We have performed a DFT theoretical description to evaluate the electronic and magnetic properties of fullerene dimers of C_{60} and C_{80} connected through C_{24} and C_{36} bridge cages with the face-to-face linking model. By comparing the results obtained in the present investigation, we emphasize the following points. First, binding energies for the fullerene dimers with C_{36} bridges are lower than those of the fullerene dimers with C_{24} bridges. Second, replacement of C_{60} cages with C_{80} ones always leads to the increase of binding energy in these systems. Third, HOMO-LUMO gaps, E_g, of the fullerene dimers with C_{36} bridges are larger than those of the fullerene dimers with C_{24} bridges and also replacement of C_{80} cage for C_{60} leads to larger E_g for the fullerene dimer. Fourth, variations of NICS values *versus* distances from the bridge center for the considered compounds and the parent cages indicate that dimerization of C_{60} and C_{80} fullerenes with C_{24} and C_{36} leads to a significant decrease in antiaromaticity of the antiaromatic cages C_{24} and C_{80}, and an increase in the aromaticity of the aromatic cages C_{36} and C_{60}. Finally, fullerene dimers involving the initially harshly antiaromatic C_{24} or C_{80} cages are more energetically favorable configurations than the fullerene dimers involving C_{36} and C_{60}.

Acknowledgments. Publication cost of this paper was supported by the Korean Chemical Society.

References

1. Karaulova, E. N.; Bagrii, E. I. *Russ. Chem. Rev.* **1999**, *68*, 889.
2. Dresselhaus, M. S.; Dresselhaus, G.; Eklunf, P. C. *Science of Fullerenes and Carbon Nanotubes*; Academic Press: New York, 1996.
3. Hirsch, A.; Brettreich, M.; Wudl, F. *Fullerenes: Chemistry and Reactions*; Wiley-VCH: Weinhem, Germany, 2005.
4. Chitta, R.; D'Souza, F. *J. Mater. Chem.* **2008**, *18*, 1440.
5. Kharisov, B. I.; Kharissova, O. V.; Gomez, M. J.; Mendez, U. O. *Ind. Eng. Chem. Res.* **2009**, *48*, 545.
6. Stephens, P. W.; Bortel, G.; Faigel, G.; Tegze, M.; Janossy, A.; Pekker, S.; Oszalnyi, G.; Forro L. *Nature* **1994**, *370*, 636.
7. Oszlanyi, G.; Bortel, G.; Faigel, G.; Granasy, L.; Bendele, G. M.; Stephens, P. W.; Forro, L. *Phys. Rev. B* **1996**, *54*, 11849.
8. Oszlanyi, G.; Baumgartner, G.; Faigel, G.; Forro, L. *Phys. Rev. Lett.* **1997**, *78*, 4438.
9. Bendele, G. M.; Stephen, P. W.; Prassides, K.; Vavekis, K.; Kordatos, K.; Tanigaki, K. *Phys. Rev. Lett.* **1998**, *80*, 736.
10. Wang, G.-W.; Komatsu, K.; Murata, Y.; Shiro, M. *Nature* **1997**, *387*, 583.
11. Chi, D. H.; Iwasa, Y.; Chen, X. H.; Takenobu, T.; Ito, T.; Mitani, T.; Nishibori, E.; Takata, M.; Sakata, M.; Kubozono, Y. *Chem. Phys. Lett.* **2002**, *359*, 177.
12. Ma, F.; Li, Z.-R.; Zhou, Z.-J.; Wu, D.; Li, Y.; Wang, Y.-F.; Li, Z.-S. *J. Phys. Chem. C* **2010**, *114*, 11242.
13. Segura, J. L.; Martin, N. *Chem. Soc. Rev.* **2000**, *29*, 13-25.
14. Gao, X.; Zhao, Y.; Yuan, H.; Chen, Z.; Chai, Z. *Chem. Phys. Lett.* **2006**, *418*, 24.
15. Komatsu, K.; Wang, G.-W.; Murata, Y.; Tanaka, T.; Fujiwara, K.; Yamamoto, K.; Saunders, M. *J. Org. Chem.* **1998**, *63*, 9358.
16. Miao, X.; Ren, T.; Sun, N.; Hu, J.; Zhu, Z.; Shao, Y.; Sun, B.; Zhao, Y.; Li, M. *J. Electroanal. Chem.* **2009**, *629*, 152.
17. Dragoe, N.; Shimotani, H.; Wang, J.; Iwaya, M.; De Bettencourt-Dias, A.; Balch, A. L.; Kitazawa, K. *J. Am. Chem. Soc.* **2001**, *123*, 1294.
18. Zhao, Y.; Chen, Z.; Yuan, H.; Gao, X.; Qu, L.; Chai, Z.; Xing, G.; Yoshimoto, S.; Tsutsumi, E.; Itaya, K. *J. Am. Chem. Soc.* **2004**, *126*, 11134.
19. Gao, X.; Yuan, H.; Chen, Z.; Zhao, Y. *J. Comput. Chem.* **2004**, *25*, 2023.
20. Fowler, P. W.; Mitchell, D.; Taylor, R.; Seifert, G. *J. Chem. Soc., Perkin Trans.* **1997**, *2*, 1901.
21. Dragoe, N.; Shimotani, H.; Hayashi, M.; Saigo, K.; De Bettencourt-Dias, A.; Balch, A. L.; Miyake, Y.; Achiba, Y.; Kitazawa, K. *J. Org. Chem.* **2000**, *65*, 3269.
22. Lebedkin, S.; Ballenweg, S.; Gross, J.; Taylor, R.; Krätschmer, W. *Tetrahedron Lett.* **1995**, *36*, 4971.
23. Fujitsuka, M.; Takahashi, H.; Kudo, T.; Tohji, K.; Kasuya, A.; Ito, O. *J. Phys. Chem. A* **2001**, *105*, 675.
24. Balch, A. L.; Costa, D. A.; Fawcett, W. R.; Winkler, K. *J. Phys. Chem.* **1996**, *100*, 4823.
25. Lebedkin, S.; Gromov, A.; Giesa, S.; Gleiter, R.; Renker, B.; Rietschel, H.; Kratschmer, W. *Chem. Phys. Lett.* **1998**, *285*, 210.
26. Osterodt, J.; Vögtle, F. *Chem. Commun.* **1996**, 547.
27. Fabre, T. S.; Treleaven, W. D.; McCarley, T. D.; Newton, C. L.; Landry, R. M.; Saraiva, M. C.; Strongin, R. M. *J. Org. Chem.* **1998**, *63*, 3522.
28. Dragoe, N.; Tanibayashi, S.; Nakahara, K.; Nakao, S.; Shimotani, H.; Xiao, L.; Kitazawa, K.; Achiba, Y.; Kikuchi, K.; Nojima, K. *Chem. Commun.* **1999**, 85.
29. Forman, G. S.; Tagmatarchis, N.; Shinohara, H. *J. Am. Chem. Soc.* **2002**, *124*, 178.
30. Shvartsburg, A. A.; Hudgins, R. R.; Gutierrez, R.; Jungnickel, G.; Frauenheim, T.; Jackson, K. A.; Jarrold, M. F. *J. Phys. Chem. A* **1999**, *103*, 5275.
31. Manaa, M. R. *J. Comput. Theor. Nanosci.* **2009**, *6*, 397.
32. Anafcheh, M.; Ghafouri, R. *Comput. Theor. Chem.* **2012**, *1000*, 85.
33. Fowler, P. W.; Mitchell, D.; Zerbetto, F. *J. Am. Chem. Soc.* **1999**, *121*, 3218.
34. Chen, Z.; Cioslowski, J.; Rao, N.; Moncrieff, D.; Bühl, M.; Hirsch, A.; Thiel, W. *Theor. Chem. Acc.* **2001**, *106*, 364.
35. Buéhl, M.; Thiel, W.; Jiao, H.; Schleyer, P. V. R.; Saunders, M.; Anet, F. A. L. *J. Am. Chem. Soc.* **1994**, *116*, 6005.
36. Chen, Z.; King, R. B. *Chem. Rev.* **2005**, *105*, 3613.

37. Schleyer, P. v. R.; Maerker, C.; Dransfeld, A.; Jiao, H.; van Eikema Hommes, N. J. R. *J. Am. Chem. Soc.* **1996**, *118*, 6317.
38. Bühl, M.; Hirsch, A. *Chem. Rev.* **2001**, *101*, 1153.
39. Frisch, M. J.; Trucks, G. W.; Schlegel, H. B.; Scuseria, G. E.; Robb, M. A.; Zakrzewski Cheeseman, J. R. V. G.; Montgomery, J. A., Jr.; Stratmann, R. E.; Burant, J. C.; Dapprich, S.; Millam, J. M.; Daniels, A. D.; Kudin, K. N.; Strain, M. C.; Farkas, O.; Tomasi, J.; Barone, V.; Cossi, M.; Cammi, R.; Mennucci, B.; Pomelli, C.; Adamo, C.; Clifford, S.; Ochterski, J.; Petersson, G. A.; Ayala, P. Y.; Cui, Q.; Morokuma, K.; Malick, D. K.; Rabuck, A. D.; Raghavachari, K.; Foresman, J. B.; Cioslowski, J.; Ortiz, J. V.; Baboul, A. G.; Stefanov, B. B.; Liu, G.; Liashenko, A.; Piskorz, P.; Komaromi, I.; Gomperts, R.; Martin, R. L.; Fox, D. J.; Keith, T.; Al-Laham, M. A.; Peng, C. Y.; Nanayakkara, A.; Gonzalez, C.; Challacombe, M.; Gill, P. M. W.; Johnson, B.; Chen, W.; Wong, M. W.; Andres, J. L.; Gonzalez, C.; Head-Gordon, M.; Replogle, E. S.; Pople, J. A., Gaussian, 98, Gaussian. Inc., Pittsburgh, PA, 1998.
40. Hariharan, P. C.; Pople, J. A. *Mol. Phys.* **1974**, *27*, 209.
41. Zhang, Y.; Wu, A.; Xu, X.; Yan, Y. *J. Phys. Chem. A* **2007**, *111*, 9431.
42. Hale, P. D. *J. Am. Chem. Soc.* **1986**, *108*, 6087.
43. Scuseria, G. E. *Chem. Phys. Lett.* **1991**, *176*, 423.
44. Fokin, A. A.; Jiao, H.; Schleyer, P. v. R. *J. Am. Chem. Soc.* **1998**, *120*, 9364.
45. Lu, X.; Chen, Z. *Chem. Rev.* **2005**, *105*, 3643.
46. Anafcheh, M.; Ghafouri, R. *Comput. Theor. Chem.* **2013**, *1017*, 1.
47. Fowler, P. W.; Heine, T.; Rogers, K. M.; Sandall, J. P. B.; Seifert, G.; Zerbetto, F. *Chem. Phys. Lett.* **1999**, *300*, 369.
48. Rivelino, R.; de Brito Mota, F. *Nano Lett.* **2007**, *7*, 1526.
49. Li, S. *Semiconductor Physical Electronics*, 2nd ed.; Springer, USA, 2006.
50. Ghafouri, R.; Anafcheh, M. *Physica E* **2012**, *44*, 1386.